Brain Tumor Pathology (2019) 36:112–120
https://doi.org/10.1007/s10014-019-00346-x

ORIGINAL ARTICLE

MN1 rearrangement in astroblastoma: study of eight cases and review of literature

Radhika Mhatre[1] · Harsha S. Sugur[1] · B. N. Nandeesh[1] · Yasha Chickabasaviah[1] · J. Saini[2] · Vani Santosh[1]

Received: 19 February 2019 / Accepted: 6 May 2019 / Published online: 20 May 2019

Abstract

Astroblastomas are unique tumours with unresolved issues in terms of their origin, molecular biology, clinical behaviour, and response to treatment. To decipher the characteristics of this tumour, we reviewed cases histologically diagnosed as astroblastoma in our institute over the past 8 years, with immunohistochemistry, and performed fluorescence in situ hybridisation (FISH), for the newly emerged *MN1* rearrangement which was reported in central nervous system high-grade neuroepithelial tumours. The mean age at diagnosis was 18.6 years with all cases seen in females and with supratentorial localisation. The tumours showed typical circumscription and bubbly appearance on imaging. The cohort included eight cases diagnosed as astroblastoma (two low grades; six anaplastic) based on histology and proliferative index. The tumours displayed characteristic astroblastic pseudorosettes with hyalinised vascular core and variable immunopositivity for glial fibrillary acidic protein, pan cytokeratin, and epithelial membrane antigen. *MN1* break-apart by FISH was found in 5/8 of our cases (62.5%), which included 2 low-grade and 3 anaplastic tumours. Tumour recurrence was noted in three cases, with *MN1* alteration in two. We account for one of the few series to study the *MN1* rearrangement in astroblastoma and conclude that *MN1* alteration is seen in a subset of these tumours.

Keywords Astroblastoma · IHC · FISH · *MN1* · CNS-HGNET

Introduction

Astroblastoma is an inexplicable tumour in terms of its origin, biological behaviour, and existence as a distinct entity, and, hence, put under the category of 'other gliomas' in the World Health Organization (WHO) classification of central nervous system (CNS) tumours, 2016. Histologically, it is a glial neoplasm, characterised by broad, non- or slightly tapering processes radiating towards central blood vessels (astroblastic pseudorosettes) that often demonstrate sclerosis [1]. Astroblastoma predominantly affects children, adolescents, and young adults with a female preponderance, and occurs exclusively in cerebral hemispheres. It accounts for 0.45–2.8% of all gliomas [2–4]. The term astroblastoma is opined to be deceptive as these tumours are neither overtly astrocytic nor are they blastic [5, 6].

The astroblastoma terminology was put forth by Bailey and Cushing in 1926 [7]. It was further characterised by Bailey and Bucy in 1930 [8]. In the first edition of the WHO classification of CNS tumours of the year 1979, astroblastoma was included under the broad category of astrocytic tumours. In the second edition of the year 1993, it was moved to neuroepithelial tumours of uncertain histogenesis and has remained there ever since [9]. The authenticity of astroblastoma as a discrete entity is disputable due to the ambiguous nature of its cell of origin. Several theories have been put forth regarding the histogenesis of this tumour including its origin from the tanycyte, a cell with features intermediate between astrocytes and ependymal cells [1]. Bailey and Bucy proposed the existence of astroblasts which are embryonic cells representing an intermediate stage between spongioblast and astrocyte [8]. Astroblastoma shares several histological features with astrocytomas and ependymomas and, hence, prone for misdiagnosis. A definite WHO grade has not been assigned to astroblastoma due to

✉ Vani Santosh
vani.santosh@gmail.com

[1] Department of Neuropathology, National Institute of Mental Health and Neurosciences (NIMHANS), Bangalore 560029, India

[2] Department of Neuroimaging and Interventional Radiology, National Institute of Mental Health and Neurosciences (NIMHANS), Bangalore 560029, India

its rarity and uncertain biological behaviour. In the literature, this tumour has been classified as low grade, when it is well-differentiated and high grade when it exhibits malignant/anaplastic features [1].

A recent study by Sturm et al., on DNA methylation profiling of CNS primitive neuroectodermal tumour (PNET), revealed four new CNS embryonal tumour entities. One subset showed *MN1* alteration with a significant number of these tumours exhibiting astroblastoma morphology and clinical characteristics. They were classified under CNS high-grade neuroepithelial tumour (CNS-HGNET) *MN1* altered entity. The authors were of the opinion that all true phenotypic astroblastomas were molecularly consistent with *MN1* altered tumours [10]. Subsequent studies have shown *MN1* alterations in a subset of tumours with astroblastoma histomorphology [11, 12]. With this background, we reviewed the cases diagnosed as astroblastoma and further evaluated their status for *MN1* alteration.

Materials and methods

This is a retrospective study carried out on eight cases of astroblastoma diagnosed at our centre over a duration of 8 years (2011–2018). Cases operated in our hospital as well as samples received for diagnosis or second opinion from other hospitals were included in this study. The histology of these cases was reviewed and an extended immunohistochemistry panel was performed to reinforce the diagnosis. The clinical features, demographics, radio imaging findings, and follow-up details, where available, were noted from the case records. Subsequently, *MN1* rearrangement was studied by the fluorescence in situ hybridisation (FISH) technique.

Immunohistochemistry (IHC)

The various IHC markers used were Glial Fibrillary Acidic Protein (GFAP) (1:100, 6F2, Dako), Pan Cytokeratin (CK) (1:200, AE1,AE3, Thermo), Epithelial Membrane Antigen (EMA) (1:100, E29, Dako), S100 (1:1500, polyclonal, Dako), Vimentin (1:100, V9, Biogenex), Isocitrate Dehydrogenase 1 (IDH1) (1:20, H09, Dianova), ATRX (1:500, polyclonal, Sigma), p53 (1:200, DO-7, Dako), L1CAM (1:500, UJ127, Sigma), Ki-67 (1:150, MIB-1, Dako), and BRAF V600E (RTU, VE1, Ventana). IHC was performed using the Ventana Benchmark automated staining system with appropriate positive and negative controls in each run. The immunoreactivity of GFAP, CK, and EMA was semi-quantitatively graded on a scale of 0 to 3 + as follows: 0 (negative in all tumour cells), 1 + (1–25% positive cells), 2 + (26–50% positive cells), and 3 + (more than 50% positive cells), as per the study by Hirose et al. [13].

Fluorescence in situ hybridisation (FISH) for *MN1* rearrangement

FISH was performed on 4u thick sections from the formalin fixed paraffin embedded (FFPE) blocks. The slides were manually deparaffinized and treated with pre-treatment solution followed by protease buffer. They were then hybridised with the *MN1* probe overnight in a ThermoBriteTM hybridisation chamber (Vysis) at 37 °C. Dual coloured *MN1* Break-Apart FISH probe kit was used by Cytotest (Marketed by Life Technologies, India, Catalogue number CT-PAC112-10-OG). CytoOrange labelled Locus Specific Probe (LSP) *MN1* 5′ end and CytoGreen labelled LSP *MN1* 3′ end. Nuclei were counterstained with 4′,6-diamidino-2-phenylindole (DAPI). Slides were viewed under fluorescence microscope (Olympus U-LH100HG) and images taken using Genasis Applied Spectral Imaging software. A minimum of 100 intact tumour nuclei were evaluated. Positive rearrangement was considered when > 20% nuclei showed abnormal signal. Medulloblastoma was used as negative control (*MN1* intact).

Results

Clinical characteristics

In the eight cases of astroblastoma, the mean age at diagnosis was 18.6 years (range 10–27 years). All the cases were females and tumours were supratentorial in location either in the frontal (3/8), parietal (3/8), fronto-parietal (1/8), or parieto-occipital (1/8) locations. The details of the cohort are shown in Table 1. The most common symptom at presentation was headache. Others included seizures, paralysis, nausea, and vomiting.

Magnetic resonance imaging (MRI) findings (Fig. 1)

MRI available in 5/8 cases revealed a supratentorial well-demarcated tumour with solid and cystic components in all cases. The lesions were hyperintense on T2-weighted images (Fig. 1a) and appeared predominantly hypointense to isointense on T1-weighted images (Fig. 1b). Susceptibility weighted imaging (SWI) showed areas of abundant susceptibility within the lesions which was likely due to old haemorrhages or presence of calcifications (Fig. 1c). Diffusion weighted imaging (DWI) and apparent diffusion coefficient (ADC) map showed restriction within the solid portion of the lesion (Fig. 1d, e). Post-contrast image showed heterogeneous enhancement (Fig. 1f). MR

Table 1 Details of the patient cohort of astroblastoma (Clinical, histology, IHC, FISH for *MN1,* and follow-up)

Case no.	Age	Sex	Location	Symptoms	Radiology	Primary tumour characteristics	GFAP	CK	EMA	FISH *MN1*	Post-operative radiotherapy	Follow-up	Histology on recurrence
1	16	F	Fronto-parietal	Headache, vomiting	Lobulated lesion, heterogeneous enhancement, elevated choline, reduced NAA, diffusion restriction, increased perfusion	Astroblastoma, mitosis 2–3/10 HPF	2 +	2 +	2 +	Break-apart	Given	AWD	–
2	23	F	Parietal	Headache	NA	Anaplastic astroblastoma, mitosis 6–7/10HPF	1 +	1 +	2 +	Break-apart	NA	NA	–
3	15	F	Parieto-occipital	Headache, vomiting, seizures	Lobulated lesion with blooming, contrast enhancing, diffusion restriction, increased perfusion	Anaplastic astroblastoma, mitosis 6–7/10 HPF	2 +	2 +	1 +	Monosomy	Given	Recurrence at 23 months. AWD	Anaplastic astroblastoma, increased cellularity, anaplasia, mitosis 7–8/10 HPF, necrosis
4	14	F	Parietal	Headache	NA	Astroblastoma, mitosis 3/10 HPF	2 +	2 +	3 +	Break-apart	NA	NA	–
5	27	F	Frontal	Headache, seizures	Multiloculated solid cystic lesion, contrast enhancing, elevated choline, reduced NAA	Anaplastic astroblastoma, mitosis 6–8/10 HPF	0	2 +	3 +	Break-apart	Given	Recurrence at 12, 34, 48, 63, 76 months. AWD	Anaplastic astroblastoma, increased cellularity, anaplasia, mitosis 9–10/10 HPF, necrosis
6	10	F	Parietal	Weakness, decreased sensation	Lobulated lesion with blooming, heterogeneous enhancement, diffusion restriction, increased perfusion	Anaplastic astroblastoma, mitosis 6/10 HPF, necrosis	0	2 +	2 +	Break-apart	Given	Recurrence at 16, 84 months. AWD	Anaplastic astroblastoma, undifferentiated cells, blurring of papillary architecture, mitosis 8–9/10 HPF, necrosis
7	23	F	Frontal	Headache, vomiting, weakness	NA	Anaplastic astroblastoma, mitosis 6/10 HPF, necrosis	2 +	0	2 +	Intact	NA	NA	–
8	21	F	Frontal	Headache, vomiting	Solid cystic lesion with internal enhancing nodule	Anaplastic astroblastoma, mitosis 8/10HPF, necrosis	1 +	1 +	3 +	Intact	NA	NA	–

Semi-quantitative grading scale used: 0 (negative in all tumour cells), 1 + (1–25% positive cells), 2 + (26–50% positive cells), and 3 + (51–100% positive cells)

F, female; NA, not available; HPF, high power field; AWD, alive with disease; IHC, immunohistochemistry; FISH, fluorescence in situ hybridization; *MN1*, Meningioma 1 gene

spectroscopy was carried out in two of these cases. In both cases, the tumour showed elevated choline and markedly reduced NAA (Fig. 1g). Perfusion imaging showed (Fig. 1h) increased relative cerebral blood volume (rCBV) within the lesion.

Microscopy (Fig. 2)

On light microscopy, the tumours showed sharp circumscription and pushing borders with cells arranged in astroblastic pseudorosettes (Fig. 2a). Cells were elongated with abundant eosinophilic cytoplasm having single stout process extending to central blood vessel showing hyaline sclerosis (Fig. 2b). In some cases, the tumours demonstrated paucicellular zones with characteristic stromal fibrosclerosis and large areas of fibrous overgrowth (Fig. 2c). They typically lacked gliofibrillary stroma. Our cohort had two cases of low-grade astroblastoma with mitosis ranging between 2 and 3/10 HPF. One case showed dystrophic calcification. The tumours with increased mitosis (> 5/10 HPF) were classified as anaplastic astroblastoma which constituted 6 cases in our study (Table 1). These tumours demonstrated increased cellularity, conspicuous mitosis (Fig. 2h), cytologic atypia, foci of necrosis, and areas with breakdown of the orderly perivascular arrangement. One case of anaplastic astroblastoma harboured trabecular pattern (Fig. 2g) with vascular sclerosis. Two of these tumours on recurrence showed marked anaplasia (Fig. 2i), brisk mitosis, necrosis, and loss of papillary pattern.

Immunohistochemistry (Fig. 2d–f)

On IHC, the cases showed variable and patchy positivity for GFAP, CK, and EMA based on our scoring criteria, as shown in Table 1. GFAP staining was variable and patchy (0 to 2+, Fig. 2d). A similar staining pattern was noted for S100 with 2 tumours being negative for both. CK immunopositivity (0 to 2+) and EMA membrane positivity (1+ to 3+) were noted within different areas of the tumour (Fig. 2e, f). All the cases were negative for IDH1(R132H), p53, L1CAM, and BRAF V600E, and showed ATRX retained nuclear expression. The range of MIB-1 labelling index in low-grade astroblastoma was 1–2% and 8–20% in anaplastic astroblastoma.

FISH analysis (Fig. 2m–o)

FISH analysis using *MN1* probe showed the following three patterns:

1. Break-apart (separated 2 red and 2 green signals; or one fused yellow and one red signal, with deletion of one green signal; or one fused yellow and one green signal, with deletion of one red signal) in 5/8 cases (Fig. 2m).
2. Monosomy (only one red and one green but closely placed) in 1/8 cases. This pattern was not considered as *MN1* alteration with break-apart, but as intact *MN1* locus (Fig. 2n).
3. Intact (2 fused yellow or closely placed red and green signals) in 2/8 cases (Fig. 2o).

Thus, *MN1* alteration with break-apart was seen in 5/8 cases of astroblastoma (62.5%) that included 2 low-grade and 3 anaplastic tumours. The remaining three cases showed an intact *MN1* locus. Histologically, among the cases included under the category of intact *MN1* locus, two showed characteristic astroblastic pseudorosettes with vascular sclerosis (Fig. 2j, k) and one showed pseudopapillary pattern (Fig. 2l) with broad cytoplasmic processes. In contrast to *MN1* intact tumours, these tumours did not show the paucicellular zones of stromal fibrous overgrowth.

Follow-up of patients

Patient follow-up details were available in 4/8 cases. One patient with low-grade astroblastoma (*MN1* altered) received adjuvant radiotherapy following resection and has a disease-free status for 5 years. Three patients with anaplastic astroblastoma presented with recurrences between 12 and 23 month post-surgery and were subsequently administered radiotherapy following the second resection. Two of these cases harboured the *MN1* alteration, and in both these cases, there was re-recurrence of the tumour, which was surgically resected. Both patients are currently on follow-up. Chemotherapy was not administered to any patient.

Discussion

The demographic characteristics of astroblastoma observed in this study, as seen in adolescence, and young adults with female predominance and supratentorial location are in accordance with other published studies and documented data in the literature [2, 3, 13]. They showed the distinctive histological picture with astroblastic pseudorosettes with stout processes radiating towards hyalinised and sclerosed blood vessels. Interestingly, the cases with *MN1* break-apart showed hyalinised vasculature coalescing into large areas of stromal fibrosclerosis in parts of the tumour, whereas, in cases with intact *MN1* locus, the hyalinisation was of relatively lesser degree and remained confined to the vessels. Imaging showed superficially located well-delineated tumour with characteristic bubbly appearance on MRI [14]. The "bubbly" appearance reflects the multicystic nature and

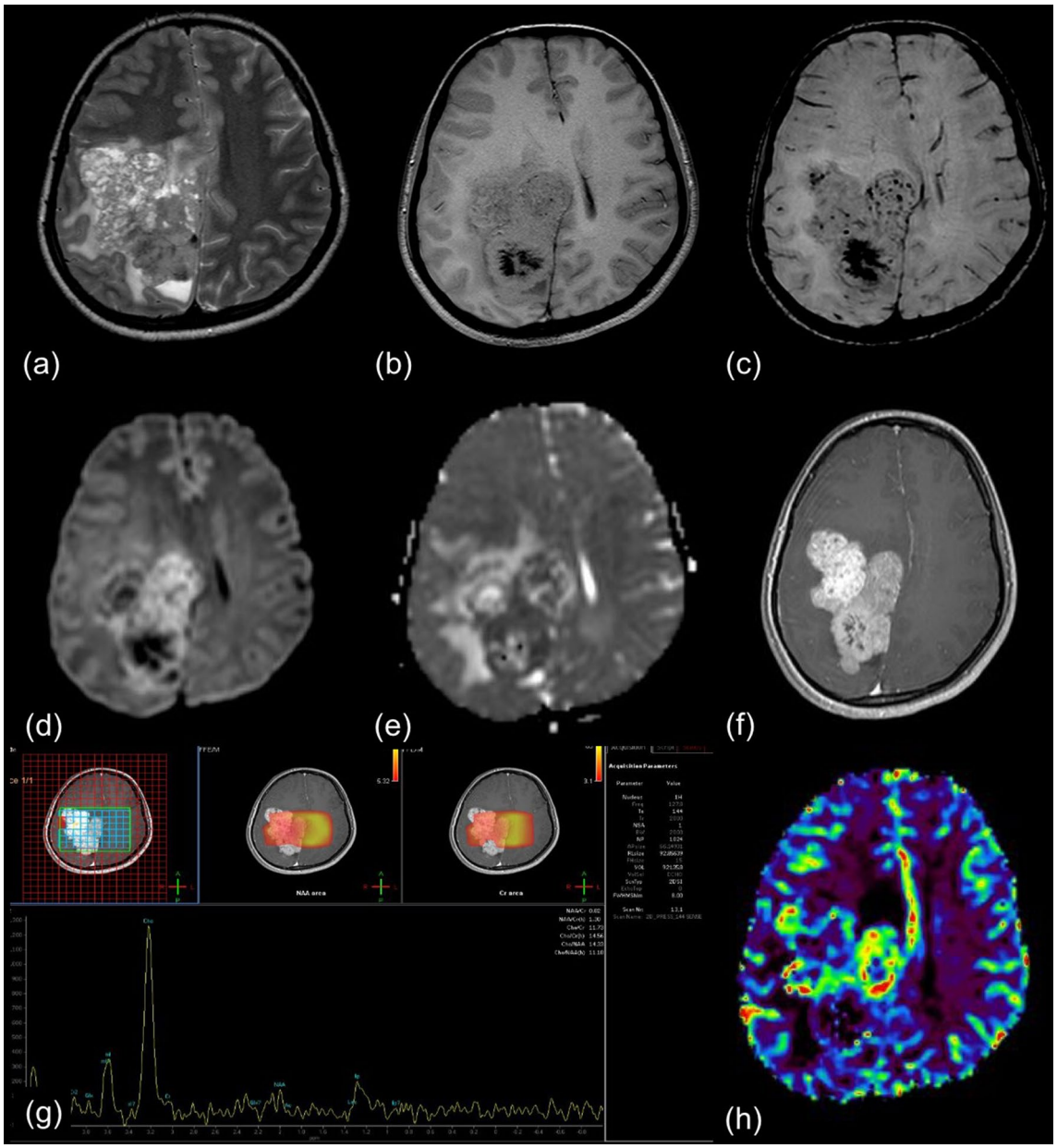

Fig. 1 Axial T2 W image (**a**) shows intra-axial T2 heterogenous lesion in right fronto-parietal location, with anterior part of the tumour showing small cystic areas which appears predominantly hypointense on T1 W image (**b**). SWI image (**c**) shows multiple microbleeds along with large area of blooming in the posterior aspect of the lesion. Diffusion weighted image (**d**) and ADC map (**e**) show diffusion restriction within the solid portion of the lesion. On post-contrast image (**f**), lesion shows strong heterogeneous enhancement. MR spectroscopy shows elevated choline and markedly reduced NAA within the lesion (**g**). Dynamic susceptibility perfusion MRI-derived CBV map (**h**) shows raised rCBV within the lesion

likely results from the angioarchitecture of the tumour causing signal voids on MRI [15].

Bonnin and Rubinstein graded astroblastomas into low grade and high grade in their study of 23 cases [6]. High-grade astroblastomas show increased cellularity, nuclear atypia, high mitotic index (> 5/10 HPF), microvascular proliferation, necrosis with pseudopalisades, and MIB-1 proliferative index varying between 6 and 22% [16]. No conspicuous relationship between proliferative index and outcome has been established, although elevated index is associated with high-grade tumour and increased risk of recurrence [1]. In our study, 6 out of 8 cases were high grade (malignant/anaplastic) based on their histology, increased proliferation index, (8–20%) and mitotic count (6–10/HPF).

IHC showed varied immunoreactivity of the tumor for GFAP, CK, and EMA, and was negative for IDH1 (R132H)

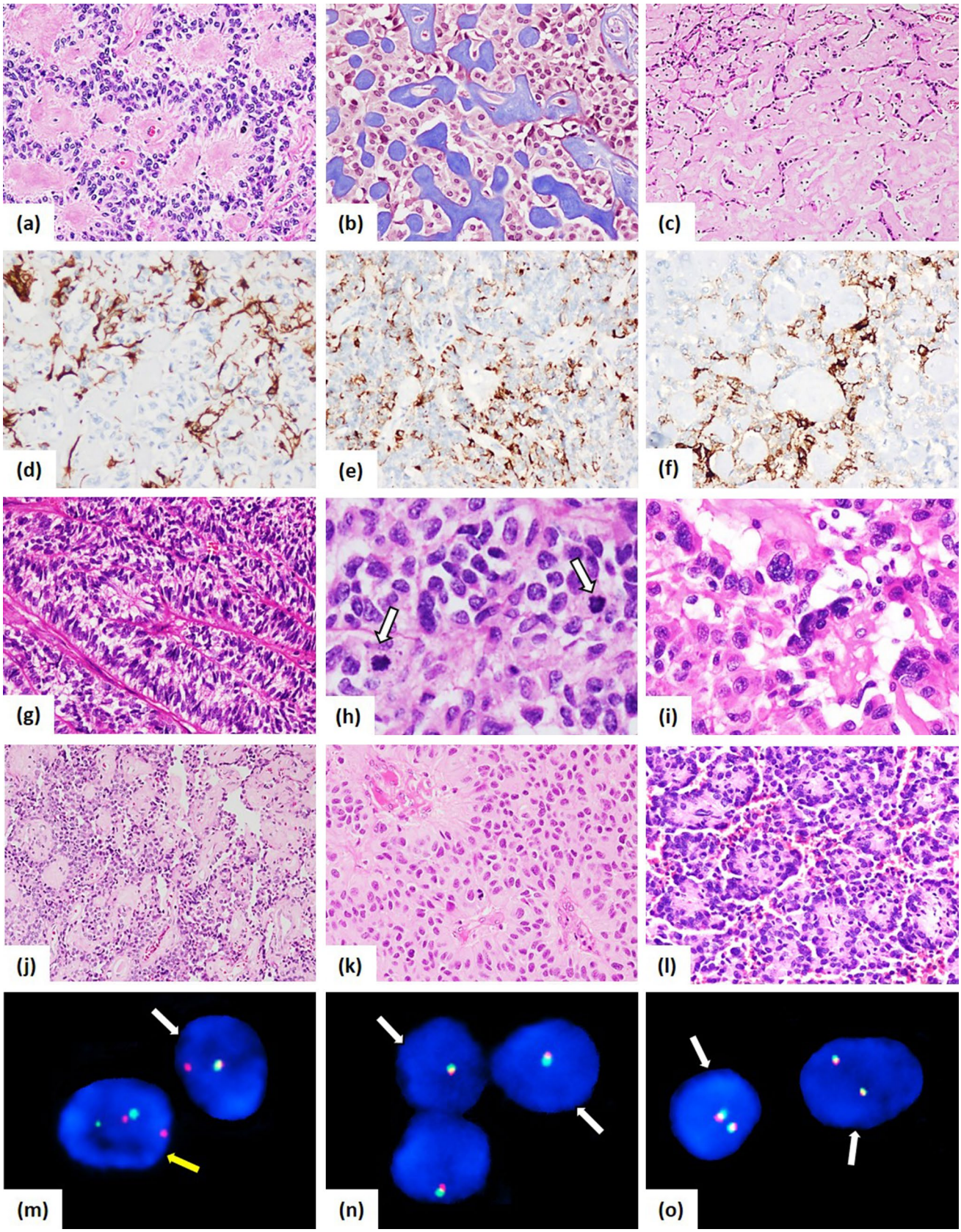
(a)
(b)
(c)
(d)
(e)
(f)
(g)
(h)
(i)
(j)
(k)
(l)
(m)
(n)
(o)

◂**Fig. 2** Microphotograph showing cells disposed in astroblastic pseudorosettes with broad non-tapering processes radiating towards central blood vessel (**a**). Hyaline sclerosis of blood vessels highlighted on Masson's trichrome stain (**b**). Stromal fibrosclerosis with large areas of fibrous overgrowth (**c**). Patchy positivity on IHC for GFAP (**d**), Pan CK (**e**), and EMA (**f**). Anaplastic astroblastoma showing trabecular pattern (**g**) and increased mitosis (**h**). Recurrent anaplastic astroblastoma with features of anaplasia (**i**). Microphotographs showing astroblastic pseudorosettes in *MN1* intact cases, with hyalinised vascular core, but lacking stromal fibrous overgrowth (**j**, **k**). Pseudopapillary pattern of arrangement (**l**). FISH for *MN1* showing break-apart (separated red and green signals—yellow arrow; one fused yellow, and one separate red signal, with deletion one corresponding green signal—white arrow) (**m**), monosomy (only one fused yellow signal or only one red and green signal but closely placed—arrows) (**n**), and intact *MN1* locus (two fused yellow signals in each nuclei—arrow) (**o**). Magnification × 100 for **c**, **j**; × 200 for **a**, **b**, **d**–**g**, **k**, **l**; × 400 for **h**, **i** and × 1000 for m–**o**. **Footnote**: **a**–**f**, represent case 1—harbouring *MN1* break-apart; **g**, **h**, represents case 5—harbouring *MN1* break-apart; i, represents case 6—harbouring *MN1* break-apart; **j**, **k** represents cases 7 and 8, respectively, harbouring intact *MN1* locus; **l** represents case 3 with monosomy of chromosome 22. GFAP, Glial fibrillary Acidic Protein; CK, Cytokeratin; EMA, Epithelial Membrane Antigen; *MN1,* Meningioma 1 gene

which is similar to other studies [3, 4, 13]. Since astroblastic pseudorosette pattern is observed in other high-grade tumours such as epithelioid glioblastoma, Hirose et al. evaluated BRAF V600E mutation in their series of astroblastomas and did not find any mutation. However, Lehman et al. found the mutation in 8 out of 21 astroblastoma cases (38%) [17]. In the present study, IHC for BRAF V600E did not reveal immunopositivity in any case, although we did not perform sequencing for BRAF mutations. Astroblastic pseudorosettes can also be seen in astrocytoma and ependymoma which are close differentials of this tumour. However, ependymomas have perivascular fibrillary processes and usually lack the hyalinised vasculature. L1CAM positivity is seen in a subset of supratentorial ependymomas which harbour the *RELA* fusion [1]. The present study showed negative immunoreactivity for L1CAM in all the tumours.

Meningioma 1 (*MN1*) gene is a transcriptional activator located on long arm (q) of chromosome 22 at position 12.1. Aberrations in *MN1* gene have been known in the pathogenesis of meningioma and acute myeloid leukemia. Recently, Sturm et al. have identified a subset of CNS high-grade neuroepithelial tumours that harbours the *MN1* alterations (CNS-HGNET-MN1). The authors noted that nearly 40% of tumours histologically diagnosed as astroblastoma belong to this category with histology showing pseudopapillary pattern and dense pericellular and vascular hyalinisation. RNA sequencing displayed two specific fusion genes in these tumours: *MN1-BEND2* and *MN1-CXXC5* [10]. Lehman et al. studied the histologically defined astroblastomas by DNA methylation profiling, and found specific genetic alterations which included *MN1* rearrangement, BRAF V600E mutations, and *RELA* rearrangement. Those which lacked the specific alterations fell into the clusters of pilocytic astrocytoma, ganglioglioma, and normal or reactive cerebrum. None of these groups could be distinguished based on histology alone, thus, concluding that histologically defined astroblastoma is a molecularly heterogenous group and not representing a single entity [12]. Similarly, Wood et al. characterised the genetic alterations that drive histologically diagnosed astroblastoma and found, in addition to *MN1* alteration, some showed features of anaplastic pleomorphic xanthoastrocytoma and IDH-wild-type glioblastoma with an aggressive course [11]. Therefore, there appears to be a significant discordance between the histology and genetics, with associated variable outcome in each of these molecular subgroups of tumours with astroblastoma morphology.

We found *MN1* break-apart by FISH in 5/8 astroblastoma cases (62.5%) that included two low-grade and three anaplastic tumours. The other three cases showed an intact *MN1* locus. The comparison of FISH *MN1* break-apart results in our study with other published studies is given in Table 2. Wood et al. in a series of eight astroblastoma cases found four cases with *MN1* break-apart by FISH. On further DNA methylation profiling, three of these cases with break-apart belonged to CNS-HGNET-MN1 class. Two others fell in line with high-grade astrocytoma and three remained unclassified [11]. On the other hand, Hirose et al. have shown *MN1* rearrangement in 100% of their cases. Array comparative genomic hybridization (CGH) was also performed by these authors in four cases which showed numerous heterozygous deletions on the X chromosome. Multiple deletions and gains were also seen near *MN1* locus [13]. In a series on 28 histologically defined astroblastomas, Lehman et al. found *MN1* alterations by FISH in eight cases with methylation class corresponding to HGNET-MN1 and in additional two cases not characterised by DNA methylation [12]. Other studies on FISH for *MN1* in astroblastoma include that by Shin et al. who reported a case of brainstem astroblastoma with *MN1* translocation in 11-year male and the case report of Yamada et al. of a 20-year female with a spinal astroblastoma showing an atypical pattern but not the classic spilt of signals on FISH [18, 19]. Other genetic alterations reported in the literature for astroblastomas are gain of 20q and 19 and losses of 9q, 10, and X by the conventional CGH [5].

Thus, a few studies in the literature have studied *MN1* alterations; however, whether *MN1* break-apart stands to be a hallmark molecular alteration of this tumour needs to be addressed. In our study, only a subset of phenotypic astroblastomas harboured the *MN1* alteration similar to study by Wood et al. [11] and Lehman et al. [12]. Hirose et al., on the other hand, found this alteration in all the cases [13]. More studies are required to clarify the

Table 2 Comparison of FISH for *MN1* break-apart with other published studies in the literature

	Wood et al. [11]	Hirose et al. [13]	Lehman et al. [12]	Present study
No of cases studied	8	8	28	8
FISH *MN1* status	4—break-apart 4—Intact	5—break-apart 2—probe did not hybridise 1—not done	10—break-apart	5—break-apart 3—intact

FISH, fluorescence in situ hybridization; *MN1*, meningioma 1 gene

defining molecular alterations of this tumour. It is plausible that the other cases with intact *MN1* locus in our study could harbour different mutations or may represent other specific molecular entities, suggesting that astroblastoma may actually be a pattern rather than a specific entity.

In our series, follow-up was available in 4/8 cases. Tumour recurrence was noted in three patients of anaplastic astroblastoma, with multiple recurrences in two of these. Both the cases showed *MN1* alteration. The recurrence pattern of the tumour in these cases connotes the aggressive behaviour of *MN1* altered anaplastic astroblastoma, although not for the low-grade *MN1* altered astroblastoma, However, our observation needs to be validated on larger cohorts of patients. Conversely, Lehman et al. have shown *MN1* rearranged astroblastomas to be associated with a favourable prognosis which was mainly in comparison to BRAF V600E mutated pleomorphic xanthoastrocytoma with astroblastoma features as categorised by DNA methylation-based classification [12]. In our study, none of the cases were immunopositive for BRAF V600E. The treatment of choice for astroblastoma is radical surgical resection. In high-grade lesions, radiotherapy may play an adjuvant role, but the benefit of chemotherapy is debatable. In view of the postulated glial origin of these tumours, the high-grade astroblastomas are to be treated aggressively with radiotherapy and subsequent temozolomide chemotherapy [16].

Conclusion

Astroblastoma is a rare, discrete entity with distinctive clinical, histological, radiological characteristics and, perhaps, genetic alterations. A subset of astroblastoma has *MN1* alterations which may belong to CNS-HGNET-MN1 entity. Those without *MN1* alteration but with astroblastoma like histology could harbour other mutations or could represent other specific genetic entities.

Acknowledgements The authors wish to acknowledge the operating neurosurgeons for referring these cases for diagnosis. We thank Mr. Chandrashekar for technical assistance and Mr. K. Manjunath for helping with the illustrations.

Funding None.

Compliance with ethical standards

Conflict of interest The authors declare no conflict of interest.

References

1. Aldape KD, Rosenblum MK, Brat DJ (2016) Astroblastoma. In: Louis DN, Ohgaki H, Wiestler OD (eds) WHO classification of tumours of the central nervous system, revised, 4th edn. IARC press, Lyon, pp 121–122
2. Brat DJ, Perry A (2018) Other glial neoplasms. In: Perry A, Brad DJ (eds) Practical surgical neuropathology. A diagnostic approach. Churchill Livingstone, Philadelphia, pp 171–182
3. Asha U, Mahadevan A, Sathiyabama D, Ravindra T, Sagar BKC, Bhat DI (2015) Lack of IDH1 mutation in astroblastomas suggests putative origin from ependymoglial cells? Neuropathology 35:303–311
4. Hammas N, Senhaji N, Lamrani MY, Bennis S, Chaoui EM, Fatemi H et al (2018) Astroblastoma—a rare and challenging tumor: a case report and review of the literature. J Med Case Repo 12:102
5. Brat DJ, Hirose Y, Cohen KJ, Feuerstein BG, Burger PC (2000) Astroblastoma: clinicopathologic features and chromosomal abnormalities defined by comparative genomic hybridization. Brain Pathol 10:342–352
6. Bonnin JM, Rubinstein LJ (1989) Astroblastomas: a pathological study of 23 tumors, with a postoperative follow-up in 13 patients. Neurosurgery 25:6–13
7. Bailey P, Cushing H (1926) A classification of the tumors of the Glioma group on a histogenetic basis with a correlated study of prognosis. JB Lippincott, Philadelphia
8. Bailey P, Bucy P (1930) Astroblastomas of the brain. Acta Psychiat Neurol 5:439–461
9. Scheithauer BW (2009) Development of the WHO classification of tumors of the central nervous system: a historical perspective. Brain Pathol 19:551–564
10. Sturm D, Orr BA, Toprak UH, Hovestadt V, Jones DTW, Capper D et al (2016) New brain tumor entities emerge from molecular classification of CNS-PNETs. Cell 164:1060–1072
11. Wood MD, Tihan T, Perry AJ et al (2018) Multimodal molecular analysis of astroblastoma enables reclassification of most cases into more specific molecular entities. Brain Pathol 28:192–202
12. Lehman NL, Usubalieva A, Lin T, Allen SJ, Tran Q, Mobley B et al (2019) Genomic analysis demonstrates that histologically-defined astroblastomas are molecularly heterogeneous and that tumors with MN1 rearrangement exhibit the most favorable prognosis. Acta Neuropathol Commun 7(1):42

13. Hirose T, Nobusawa S, Sugiyama K, Amatya V, Fujimoto N, Sasaki A et al (2018) Astroblastoma: a distinct tumor entity characterized by alterations of the X chromosome and MN1 rearrangement. Brain Pathol 28(5):684–694
14. Port JD, Brat DJ, Burger PC, Pomper MG (2002) Astroblastoma: radiologic–pathologic correlation and distinction from ependymoma. Am J Neuroradiol 23:243–247
15. Bell JW, Osborn AG, Salzman KL, Blaser SI, Jones BV, Chin SS (2007) Neuroradiologic characteristics of astroblastoma. Neuroradiology 49:203–209
16. Salvati M, D'Elia A, Brogna C, Frati A, Antonelli M, Giangaspero F et al (2009) Cerebral astroblastoma: analysis of six cases and critical review of treatment options. J Neurooncol 93:369–378
17. Lehman NL, Hattab EM, Mobley BC, Usubalieva A, Schniederjan MJ, McLendon RE et al (2017) Morphological and molecular features of astroblastoma, including BRAFV600E mutations, suggest an ontological relationship to other cortical-based gliomas of children and young adults. Neuro-oncolpgy 19:31–42
18. Shin SA, Ahn B, Kim SK, Kang HJ, Nobusawa S, Komori T et al (2018) Brainstem astroblastoma with MN1 translocation. Neuropathology 38(6):631–637
19. Yamada SM, Tomita Y, Shibui S et al (2018) Primary spinal cord astroblastoma: case report. J Neurosurg Spine 28:642–646